Clinical & Experimental Immunology
The Journal of Translational Immunology

Clinical and Experimental Immunology ORIGINAL ARTICLE doi:10.1111/cei.12120

Human adipose-tissue derived mesenchymal stem cells induce functional *de-novo* regulatory T cells with methylated *FOXP3* gene DNA

A. U. Engela, M. J. Hoogduijn, K. Boer, N. H. R. Litjens, M. G. H. Betjes, W. Weimar and C. C. Baan

Department of Internal Medicine, Section Nephrology and Transplantation, Erasmus MC, University Medical Center, Rotterdam, the Netherlands

Accepted for publication 10 April 2013
Correspondence: A. U. Engela, Erasmus MC, Department of Internal Medicine, Section Nephrology and Transplantation, PO Box 2040, Room Ee563a, 3000 CA Rotterdam, the Netherlands.
E-mail: a.grohnert@erasmusmc.nl

Summary

Due to their immunomodulatory properties, mesenchymal stem cells (MSC) are interesting candidates for cellular therapy for autoimmune disorders, graft-*versus*-host disease and allograft rejection. MSC inhibit the proliferation of effector T cells and induce T cells with a regulatory phenotype. So far it is unknown whether human MSC-induced $CD4^+CD25^+CD127^-$forkhead box P3 $(FoxP3)^+$ T cells are functional and whether they originate from effector T cells or represent expanded natural regulatory T cells (nT_{reg}). Perirenal adipose-tissue derived MSC (ASC) obtained from kidney donors induced a 2·1-fold increase in the percentage of $CD25^+CD127^-FoxP3^+$ cells within the $CD4^+$ T cell population from allostimulated $CD25^{-/dim}$ cells. Interleukin (IL)-2 receptor blocking prevented this induction. The ASC-induced T cells (iT_{reg}) inhibited effector cell proliferation as effectively as nT_{reg}. The vast majority of cells within the iTreg fraction had a methylated *FOXP3* gene Treg-specific demethylated region (TSDR) indicating that they were not of nT_{reg} origin. In conclusion, ASC induce T_{reg} from effector T cells. These iT_{reg} have immunosuppressive capacities comparable to those of nT_{reg}. Their induction is IL-2 pathway-dependent. The dual effect of MSC of inhibiting immune cell proliferation while generating *de-novo* immunosuppressive cells emphasizes their potential as cellular immunotherapeutic agent.

Keywords: immunosuppression, induction, interleukin-2 receptor signalling, mesenchymal stem cells, regulatory T cells

Introduction

Mesenchymal stem cells (MSC) can be isolated from an abundance of human tissue sites, including adipose tissue and bone marrow, and their expansion is accomplished easily [1–4]. MSC possess immunosuppressive capacities and, as a consequence, over the past decennium MSC have been studied extensively as a prospective cellular therapeutic agent to prevent or treat autoimmune diseases, graft-*versus*-host disease (GVHD) and allograft rejection [5–12]. Upon activation, MSC prevent the proliferation of various immune cells, in particular T cell proliferation [13–19]. MSC mediate their suppressive effect through cell–cell contact and the secretion of various soluble factors such as transforming growth factor (TGF)-β, hepatocyte growth factor (HGF), interleukin (IL)-10, nitric oxide (NO), human leucocyte antigen G5 (HLA-G5), indoleamine 2,3-dioxygenase (IDO) and prostaglandins [20–28]. While MSC strongly inhibit T cell proliferation via these mechanisms, they preserve the function of $CD4^+CD25^+CD127^-$forkhead box P3 $(FoxP3)^+$ regulatory T cells (T_{reg}) [29]. Beyond this, *in-vitro* studies and studies in animal models have indicated that MSC have the capacity to generate T_{reg} [9,30–34]. Recent evidence was provided that this phenomenon might also occur in renal transplant patients undergoing MSC therapy [35]. Intravenous administration of autologous MSC post-transplant led to a proportional increase of $CD4^+CD25^+CD127^-FoxP3^+$ T cells. Despite their regulatory phenotype, it remains essential to investigate the characteristics and function of these cells. Further, due to the heterogeneity of the T_{reg} population these $CD4^+CD25^+CD127^-FoxP3^+$ T cells could represent expanded natural T_{reg} (nT_{reg}) or newly induced T_{reg} (iT_{reg}).

nT_{reg} and iT_{reg} are distinct from each other with regard to their place of origin, the stability of their transcription factor *FOXP3* expression and in their methylation pattern

of the T_{reg}-specific demethylated region (TSDR) in the *FOXP3* gene [36,37]. nT_{reg} develop intrathymically, express *FOXP3* constitutively and have a fully demethylated *FOXP3* TSDR. In contrast, iT_{reg} development takes place in the periphery, their *FOXP3* expression is inducible and their *FOXP3* TSDR is fully methylated. The MSC-mediated generation of cells with an immunosuppressive function is of particular importance if one considers the fate of MSC after infusion; Eggenhofer *et al.* [38] showed recently that after intravenous administration into mice, MSC survive no longer than 24 h. This evident short lifespan of MSC in connection with their proven ability to prolong graft survival prompts further investigation to reveal how MSC accomplish long-term immunosuppression, and which mediators and mechanisms are involved in this phenomenon.

While we have studied previously the interaction between human adipose-tissue derived MSC (ASC) and natural T_{reg} [29], the aim of this study was to determine whether human ASC can generate functional *de-novo* iT_{reg} from $CD25^{-/dim}$ effector T cells and to find evidence for the mechanisms involved in MSC-mediated T_{reg} induction.

Material and methods

Origin, isolation and culture of human ASC

Perirenal adipose tissue was removed surgically from living kidney donors and collected in minimum essential medium Eagle alpha modification (MEM-α) (Sigma-Aldrich, St Louis, MO, USA) supplemented with 2 mM L-glutamine (Lonza, Verviers, Belgium), 1% penicillin/streptomycin solution (P/S; 100 IU/ml penicillin, 100 IU/ml streptomycin; Lonza). Samples were obtained with written informed consent, as approved by the Medical Ethical Committee at Erasmus University Medical Center Rotterdam (protocol no. MEC-2006-190).

ASC were isolated, cultured and characterized as described previously [29]. In brief, perirenal adipose tissue was disrupted mechanically and digested enzymatically with collagenase type IV (Life Technologies, Paisley, UK). ASC were expanded using ASC culture medium consisting of MEM-α with 2 mM L-glutamine, 1% P/S and 15% fetal bovine serum (FBS; Lonza) in a humidified atmosphere with 5% CO_2 at 37°C. Culture medium was refreshed twice weekly. At subconfluency, ASC were removed from culture flasks using 0·05% trypsin-ethylenediamine tetraacetic acid (EDTA) (Life Technologies) and reseeded at 1000 cells/cm^2. ASC were characterized by means of immunophenotyping and by their ability to differentiate into adipocytes and osteoblasts. ASC cultured between two and six passages were used. ASC from these passages did not differ in their ability to differentiate or to exert their immunosuppressive functions.

Isolation of peripheral blood mononuclear cells

Peripheral blood mononuclear cells (PBMC) were isolated from buffy coats of healthy blood donors (Sanquin, Rotterdam, the Netherlands) by density gradient centrifugation using Ficoll-Paque PLUS (density 1·077 g/ml; GE Healthcare, Uppsala, Sweden). Cells were frozen at −150°C until further use in Roswell Park Memorial Institute (RPMI)-1640 medium with GlutaMAX™-I (Life Technologies) supplemented with 1% P/S, 10% human serum (Sanquin) and 10% dimethylsulphoxide (DMSO; Merck, Hohenbrunn, Germany).

Isolation of effector cells and nT_{reg} from PBMC

$CD25^{-/dim}$ cells (effector cells) and $CD25^{bright}$ cells (nT_{reg}) were separated by means of CD25 MicroBeads II (Miltenyi Biotec, Bergisch Gladbach, Germany) and magnetic cell sorting, as described previously [29]. Cell fraction purity was determined by flow cytometry using monoclonal antibodies (mAbs) against CD3-AmCyan (clone SK7), CD4-Pacific Blue (RPA-TA), CD25-phycoerythrin (PE)-cyanin 7 (Cy7) (epitope B; M-A251), CD127-PE (HIL-7R-M21; all BD Biosciences, San Jose, CA, USA); and FoxP3-allophycocyanin (APC) (PCH101; eBioscience, San Diego, CA, USA). Intracellular FoxP3 staining was carried out following the manufacturer's instructions of the anti-human FoxP3 staining set APC (eBioscience). Flow cytometric analyses were performed using the BD FACSCanto II flow cytometer and BD FACSDiva software (both BD Biosciences).

Mixed lymphocyte reaction and suppression assay

Mixed lymphocyte reactions (MLR) consisted of 5×10^4 $CD25^{-/dim}$ effector cells stimulated with 5×10^4 γ-irradiated (40 Gy) allogeneic PBMC in round-bottomed 96-well plates (Nunc, Roskilde, Denmark) using PBMC culture medium (PCM) consisting of MEM-α supplemented with 2 mM L-glutamine, 1% P/S and 10% heat-inactivated human serum. Effector–stimulator cell combinations were chosen on the basis of a minimum of four HLA mismatches. The immunomodulatory capacities of ASC (various concentrations), nT_{reg} (1:10), ASC-induced $CD4^+CD25^+CD127^-$ T cells (1:10) and control $CD4^+CD25^-$ T cells (1:10) (all ratios: indicated cells/effector cells) on the MLR were determined in suppression assays. After an 8-h incubation period on day 7, [^{3}H]-thymidine incorporation (0·25 μCi/well; PerkinElmer, Groningen, the Netherlands) was measured using the Wallac 1450 MicroBeta TriLux (PerkinElmer). When MLR were performed in microtitre plates with different well sizes, the number of cells was adjusted accordingly. When applicable, 50 μl cell-culture supernatant was harvested prior to the addition of [^{3}H]-thymidine and frozen at −80°C until further use.

Induction of $CD4^+CD25^+CD127^-FoxP3^+$ T cells by ASC

$CD25^{-/dim}$ effector cells were labelled using the PKH67 Green Fluorescent Cell Linker Kit (Sigma-Aldrich). For discrimination, allogeneic stimulator PBMC were labelled with PKH26 (PKH26 Red Fluorescent Cell Linker Kit; Sigma-Aldrich), according to the manufacturer's instructions. MLR were performed for 7 days in the absence or presence of ASC (1:40; ASC/effector cells). The PKH-label dilution caused by proliferation was measured by flow cytometry. After a 7-day incubation period in the absence or presence of 4 μg/ml basiliximab (Novartis Pharma, Nürnberg, Germany), cells were stained with mAbs against CD3-AmCyan (clone SK7), CD4-Pacific Blue (RPA-TA), CD8-peridinin chlorophyll (PerCP) (SK1), CD25-APC-Cy7 (epitope B; M-A251) and CD127-PE-Cy7 (HIL-7R-M21; all BD Biosciences) and FoxP3-APC (PCH101; eBioscience). Allogeneic stimulator PBMC were excluded from the analysis based on their PKH26-label. To confirm that basiliximab does not interfere with the binding of the monoclonal anti-CD25 antibody on epitope B, a competition staining was performed. In the presence of basiliximab no weakening of the CD25 staining was observed.

Isolation and function test of ASC-induced $CD4^+CD25^+CD127^-$ T cells

ASC-induced $CD4^+CD25^+CD127^-$ T cells were generated in primary MLR consisting of $CD25^{-/dim}$ effector cells and allogeneic stimulator PBMC in the presence or absence of ASC (1:40; ASC/effector cells). Allogeneic stimulator PBMC were labelled with PKH67 (Sigma-Aldrich). After 7 days, cells were stained with mAbs against CD3-AmCyan (clone SK7), CD4-Pacific Blue (RPA-TA), CD25-PE-Cy7 (epitope B; M-A251), CD127-PE (HIL-7R-M21) and BD Via-Probe™ (7-AAD-PerCP) (all BD Biosciences). ASC-induced T_{reg} were defined as $PKH67^-7\text{-}AAD^-CD3^+CD4^+CD25^+CD127^-$ cells. Cell sorting was performed using the BD FACSAria II cell sorter (BD Biosciences).

Sorted $PKH67^-7\text{-}AAD^-CD3^+CD4^+CD25^+CD127^-$ cells (1:10) were reseeded into secondary MLR. $PKH67^-7\text{-}AAD^-CD3^+CD4^+CD25^-$ cells (1:10) were used as negative control; nT_{reg} (1:10) obtained from PBMC by magnetic cell separation served as positive control (all ratios: indicated cells/effector cells). After an 8-h incubation period on day 7, [^{3}H]-thymidine incorporation (0·25 μCi/well; PerkinElmer) was measured. Alternatively, sorted cell samples were washed twice with phosphate-buffered saline-diethylpyrocarbonate (PBS-DEPC) and frozen at −80°C until further use.

Quantitative DNA methylation analysis of the *FOXP3* gene TSDR

To quantify DNA methylation of the *FOXP3* gene TSDR, the EZ DNA Methylation-Direct™ Kit (Zymo Research, Irvine, CA, USA) was used according to the manufacturer's instructions. Cell pellets were digested with proteinase K prior to bisulphite conversion. During DNA bisulphite treatment, unmethylated cytosines are converted into uracils while methylated cytosines remain unmodified. After bisulphite treatment, the TSDR of the *FOXP3* gene was amplified by quantitative real-time PCR (qPCR) using the StepOnePlus™ real-time PCR system and the TaqMan® Genotyping Master Mix (all Applied Biosystems). Methylation-specific and demethylation-specific amplification primers and probes were chosen as suggested by Wieczorek *et al*. [39]. The percentage of cells within a cell fraction with a methylated TSDR was calculated using the ratio of amplified methylated TSDR copies and the sum of amplified methylated and unmethylated TSDR copies. To correct for the X-linked nature of the *FOXP3* gene, results obtained from female PBMC donors were multiplied by 2. Intra- and interassay variations were determined by negative controls and positive reference samples.

Flow cytometric characterization of $CD4^+CD25^+CD127^-FoxP3^+$ T cells and $CD4^+CD25^+FoxP3^-$ T cells

The induction of $CD4^+CD25^+CD127^-FoxP3^+$ T cells by ASC (1:40; ASC/effector cells) was initiated as described above. Allogeneic stimulator PBMC were labelled with either PKH67 or BD Horizon Violet Cell Proliferation Dye 450 (VPD450; BD Biosciences). After 7 days, cells were stained with mAbs against CD3-AmCyan (clone SK7), CD4-PerCP (SK3), CD25-APC-Cy7 (epitope B; M-A251), CD127-PE-Cy7 (HIL-7R-M21), cytotoxic T lymphocyte antigen-4 (CTLA-4)-APC (BNI3; all BD Biosciences), glucocorticoid-induced TNFR-related protein (GITR)-fluorescein isothiocyanate (FITC) (110416; R&D Systems Europe Ltd, Abingdon, UK), Helios-Pacific Blue (22F6; BioLegend, San Diego, CA, USA) and FoxP3-PE or FoxP3-APC (both PCH101; eBioscience). Fluorescence minus one (FMO) controls were used to determine negative expression.

mRNA expression analysis

ASC were cultured alone or co-cultured with MLR (1:5; ASC/effector cells) for 7 days. In co-cultures, MLR were separated from ASC by cell culture inserts with permeable membrane supports (0·4 μm pore size; Greiner Bio-One, Alphen a/d Rijn, the Netherlands). ASC were harvested and washed twice with PBS-DEPC. Cells were either handled immediately or snap-frozen in liquid nitrogen and stored at −80°C. Total RNA was purified using the High Pure RNA Isolation Kit (Roche Diagnostics), according to the manufacturer's instructions. Complementary DNA (cDNA) was synthesized by reverse transcription using random primers. qPCR was performed using 500 ng cDNA, the

StepOnePlus™ real-time PCR system, TaqMan Universal PCR Master Mix and the assay-on-demand primer/probes for IL-2 (Hs00174114.m1) (Applied Biosystems, Foster City, CA, USA). Glyceraldehyde-3-phosphate dehydrogenase (GAPDH) mRNA served as endogenous control for normalization (Hs99999905.m1; Applied Biosystems). Intra- and interassay variations were determined by negative controls and positive reference samples. Changes in target gene expression relative to the GAPDH gene were quantified using the comparative C_T method [40]. Fold changes fewer than three were considered insignificant.

Cytometric bead array (CBA)

Supernatants were obtained from ASC cultures, MLR and ASC-MLR co-cultures (1:40; ASC/effector cells) in the absence or presence of 4 μg/ml basiliximab (Novartis Pharma) after a 7-day incubation period. They were frozen until further use at −80°C. IL-2 concentrations were measured using the BD cytometric bead array human T helper type 1 (Th1)/Th2/Th17 Cytokine Kit (BD Biosciences), according to the manufacturer's instructions.

Flow cytometric analysis of IL-2 expression by $CD4^+CD25^+CD127^-FoxP3^+$ T cells and $CD4^+CD25^+FoxP3^-$ T cells

$CD4^+CD25^+CD127^-FoxP3^+$ T cells were induced by ASC (1:40; ASC/effector cells) as described above. $CD25^{-/dim}$ effector cells were labelled with VPD450 (BD Biosciences). For discrimination, allogeneic stimulator PBMC were labelled with PKH67 (Sigma-Aldrich). MLR were performed in the absence or presence of ASC and 4 μg/ml basiliximab (Novartis Pharma). After 7 days, cells were stimulated with 50 ng/ml phorbol 12-myristate 13-acetate (PMA) and 1 μg/ml calcium ionomycin (both Sigma-Aldrich) in the presence of BD GolgiStop (BD Biosciences) for 4 h. Subsequently cells were stained with mAbs against CD3-AmCyan (clone SK7), CD4-PerCP (SK3), CD25-APC-Cy7 (epitope B; SK1), CD127-PE-Cy7 (HIL-7R-M21), IL-2-APC (5344.111; all BD Biosciences) and FoxP3-PE (PCH101; eBioscience). FMO controls were used to determine negative expression.

Statistical analysis

Statistical analyses were performed by means of one-way analysis of variance (ANOVA), Bonferroni's multiple comparison tests and (un)paired *t*-tests using GraphPad Prism 5 software (GraphPad Software, San Diego, CA, USA). A *P*-value lower than 0·05 was considered statistically significant. Two-tailed *P*-values are stated.

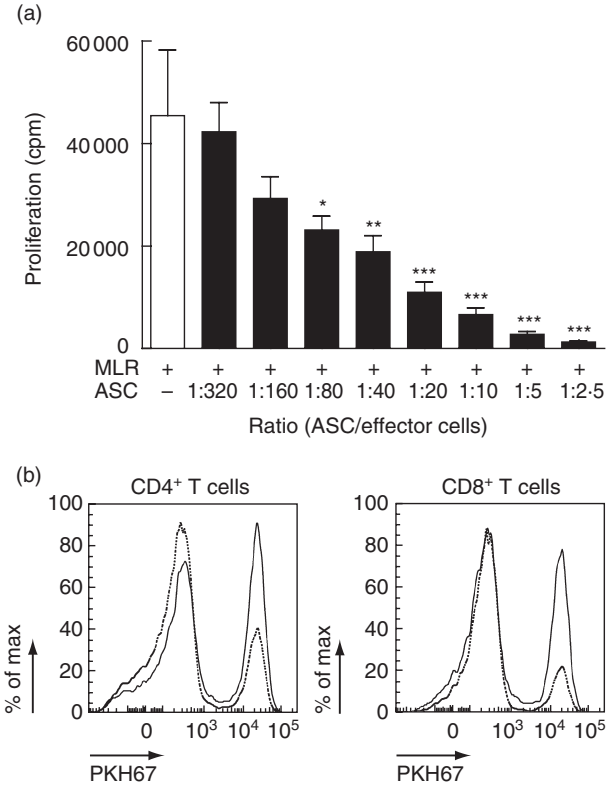

Fig. 1. Effect of adipose-tissue derived mesenchymal stem cells (ASC) on the proliferation of alloactivated $CD25^{-/dim}$ cells. (a) Mixed lymphocyte reaction (MLR) (white bar) consisted of $CD25^{-/dim}$ effector cells stimulated with γ-irradiated allogeneic peripheral blood mononuclear cells (PBMC) with a minimum of four human leucocyte antigen (HLA)-mismatches. MLR were performed in the presence of various ASC concentrations for 7 days ($n = 9$, mean ± standard error of the mean, one-way ANOVA: $P < 0{\cdot}0001$). The Bonferroni multiple comparison test was used to compare the different conditions with the MLR condition. $^*P < 0{\cdot}05$; $^{**}P < 0{\cdot}01$; $^{***}P < 0{\cdot}001$. (b) Proliferation of $CD4^+$ T cells and $CD8^+$ T cells in a 7-day MLR in the absence (dotted histograms) and presence of ASC (1:40 ratio, ASC/effector cells; solid histograms) was tracked using PKH67-labelling.

Results

ASC inhibit the proliferation of $CD25^{-/dim}$ effector cells dose-dependently and induce $CD4^+CD25^+CD127^-FoxP3^+$ T cells

The immunosuppressive effect of ASC on the proliferation of $CD25^{-/dim}$ effector cells was examined by means of [^{3}H]-thymidine incorporation. $CD25^{-/dim}$ effector cells were stimulated with γ-irradiated allogeneic PBMC for 7 days resulting in a strong proliferative activity of these cells (Fig. 1a). Co-culture with third-party ASC suppressed the effector cell proliferation in a dose-dependent manner (one-way ANOVA, $P < 0{\cdot}0001$), confirming our previously

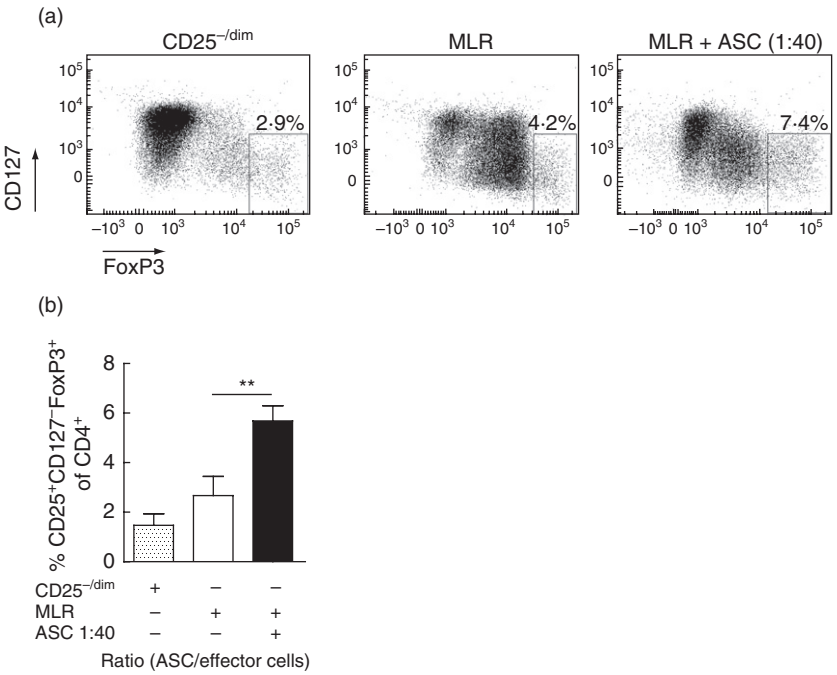

Fig. 2. Effect of adipose-tissue derived mesenchymal stem cells (ASC) on the induction of $CD4^+CD25^+CD127^-$forkhead box P3 $(FoxP3)^+$ T cells. Mixed lymphocyte reaction (MLR) (white bar) consisted of $CD25^{-/dim}$ effector cells stimulated with γ-irradiated allogeneic peripheral blood mononuclear cells (PBMC) and were performed for 7 days. In MLR co-cultures ASC were used at a 1:40 ratio (ASC/effector cells). The percentage of $CD25^+CD127^-FoxP3^+$ cells within the $CD4^+$ T cell population was determined by flow cytometry. (a) Representative examples are shown. (b) Data of multiple experiments are shown. $n = 6$, mean ± standard error of the mean; paired *t*-test; $^{**}P < 0{\cdot}01$.

published data [29]. ASC reduced significantly the proliferation from a ratio of 1:80 (ASC/effector cells). ASC suppressed the proliferation of $CD4^+$ T cells and $CD8^+$ T cells (Fig. 1b).

The effect of ASC on the generation of $CD4^+CD25^+CD127^-FoxP3^+$ T cells from $CD25^{-/dim}$ cells was determined by flow cytometry. At a 1:40 ratio, ASC reduced the proliferation of $CD25^{-/dim}$ effector cells by 59% (Fig. 1a) and mediated a 2·1-fold increase in the percentage of $CD25^+CD127^-FoxP3^+$ cells within the $CD4^+$ T cell population (Fig. 2).

ASC-induced $CD4^+CD25^+CD127^-$ T cells are immunosuppressive

The suppressive capacity of ASC-induced $CD4^+CD25^+CD127^-$ T cells was determined by means of $[^3H]$-thymidine incorporation and compared to the effect of nT_{reg}. Sorted ASC-induced $CD4^+CD25^+CD127^-$ T cells (median purity: 98·7%; range 95·3%–99·7%) were added at a 1:10 ratio to secondary MLR. They inhibited the proliferation of $CD25^{-/dim}$ effector cells as effectively as nT_{reg} (1:10; 61% suppression *versus* 48%, respectively; $P = 0{\cdot}402$; Fig. 3). Hence, ASC induce functional regulatory T cells. MLR-induced $CD4^+CD25^+CD127^-$ T cells (median purity: 99·5%; range 98·5–99·8%) also suppressed proliferation (1:10; 87%). Sorted $CD4^+CD25^-$ T cells from an MLR or MLR–ASC co-culture (1:10; median purities 99·8 and 99·7%; ranges 99·5–99·8% and 99·3–99·9%), as negative controls, did not inhibit the proliferative activity of the effector cells.

Functional ASC-induced $CD4^+CD25^+CD127^-$ T_{reg} are *de-novo* cells

To determine the origin of the ASC-induced T_{reg}, i.e. iT_{reg} or nT_{reg}, the methylation status of the TSDR was investigated. The percentage of cells with a methylated *FOXP3* gene TSDR present in different cell fractions was determined by means of quantitative DNA methylation analysis. The $CD25^{-/dim}$ fraction, obtained from PBMC by magnetic cell separation, consisted almost entirely (98·1%) of cells with a methylated *FOXP3* TSDR (Fig. 4a). In contrast, the nT_{reg} fraction consisted to 67·3% of cells with a demethylated *FOXP3* TSDR, confirming their thymic origin. After 7-day MLR in the presence of ASC (1:40; ASC/effector cells) using allostimulated $CD25^{-/dim}$ cells as effector cells, sorted fractions of $CD4^+CD25^+CD127^-$ iT_{reg} and $CD4^+CD25^-$ T cells contained 83·7 and 99·9% cells with a methylated *FOXP3* TSDR, respectively. The small percentage of cells (16·3%) with a demethylated *FOXP3* TSDR in the $CD4^+CD25^+CD127^-$ iT_{reg} fraction probably represents proliferated nT_{reg} which were present in the initial $CD25^{-/dim}$ fraction (1·9%). This demonstrates that ASC expand nT_{reg}, but that the majority of the $CD4^+CD25^+CD127^-$ T_{reg} found after 7-day MLR–ASC co-culture are induced from $CD25^{-/dim}$ cells.

To characterize further the ASC-induced $CD4^+CD25^+CD127^-FoxP3^+$ T_{reg} (Fig. 4b), their expression of GITR, CTLA-4 and Helios was investigated (Fig. 4c,d). While the expression levels of GITR were similar for iT_{reg} and $CD4^+CD25^+FoxP3^-$ T cells, iT_{reg} showed the tendency to have higher Helios levels and expressed 3·2-fold more CTLA-4 than $FoxP3^-$ T cells ($P = 0{\cdot}003$).

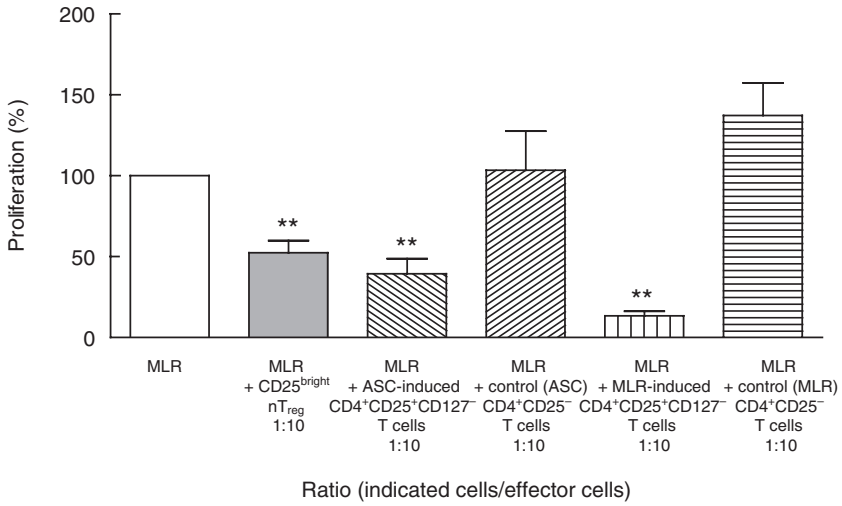

Fig. 3. Effect of adipose-tissue derived mesenchymal stem cells (ASC)-induced $CD4^+CD25^+CD127^-$ T cells on the proliferation of alloactivated $CD25^{-/dim}$ effector cells. Primary mixed lymphocyte reaction (MLR) consisted of $CD25^{-/dim}$ effector cells stimulated with γ-irradiated allogeneic peripheral blood mononuclear cells (PBMC). For the induction of $CD4^+CD25^+CD127^-$ T cells, ASC (1:40; ASC/effector cells) were added to primary MLR. After an incubation period of 7 days, $CD4^+CD25^+CD127^-$ T cells and $CD4^+CD25^-$ T cells were separated from the total lymphocyte populations from MLR or ASC–MLR co-cultures by cell sorting and added to secondary MLR at a 1:10 ratio (indicated cells/effector cells). $CD25^{bright}$ natural regulatory T cells (nT_{reg}) (1:10) were incubated with the same MLR to compare the function of the sorted fractions to the suppressive function of nT_{reg}. For statistical analyses, the MLR condition was used as reference. $n = 4$, mean ± standard error of the mean; paired *t*-test; $^{**}P < 0{\cdot}01$.

The induction of $CD4^+CD25^+CD127^-FoxP3^+$ T_{reg} by ASC coincides with increased IL-2 levels and is IL-2 pathway-dependent

IL-2 is known to be required for the expansion and function of nT_{reg}. Therefore, its involvement in the ASC-mediated induction of $CD4^+CD25^+CD127^-FoxP3^+$ T_{reg} was investigated (Fig. 5). Seven-day MLR were cultured in the absence or presence of ASC (1:40; ASC/effector cells) and concentrations of secreted IL-2 in the supernatant were analysed. IL-2, 20·1 pg/ml, was detected in the supernatant of an MLR of $CD25^{-/dim}$ effector cells stimulated with allogeneic PBMC. Non-activated ASC and MLR-activated ASC do not express IL-2 (data not shown). However, activated ASC mediated a 15·1-fold increase in IL-2 levels by effector cells during MLR suppression and induction of $CD4^+CD25^+$ $CD127^-FoxP3^+$ T_{reg}. The monoclonal anti-IL-2 receptor antibody basiliximab (4 μg/ml) effectively inhibited the IL-2 consumption in MLR and MLR–ASC co-cultures (1:40; ASC/effector cells; Fig. 5a); in the presence of basiliximab IL-2 concentrations in MLR and MLR–ASC co-cultures accumulated to 217 and 525 pg/ml, respectively.

To gain knowledge regarding which cell subset contributed most to the IL-2 concentrations detected in the supernatant, the percentage of IL-2-expressing cells within the $CD4^+CD25^+CD127^-FoxP3^+$ iT_{reg} and $CD4^+CD25^+FoxP3^-$ T cells was investigated. The majority of the IL-2-expressing cells were $CD4^+CD25^+FoxP3^-$ T cells (Fig. 5b,c). The IL-2 levels produced were similar between the IL-2 expressing $CD4^+CD25^+CD127^-FoxP3^+$ iT_{reg} and $CD4^+CD25^+FoxP3^-$ T cells (Fig. 5d).

To examine the effect of the IL-2 pathway on the ASC-mediated generation of functional $CD4^+CD25^+CD127^-$ $FoxP3^+$ iT_{reg} from $CD25^{-/dim}$ cells, IL-2 binding to its receptor was blocked with basiliximab. MLR were performed for 7 days in the absence and presence of ASC (1:40; ASC/effector cells). Basiliximab reduced the percentage of $CD25^+CD127^-$ $FoxP3^+$ cells within the $CD4^+$ T cell population (Fig. 6). In the presence of basiliximab, ASC did not induce a proportional increase of $CD25^+CD127^-FoxP3^+$ cells within the $CD4^+$ T cell population.

Discussion

Knowledge about the underlying mechanisms of how ASC contribute to a reduced responsiveness of immune effector cells is scarce. The present study provides the first evidence that human ASC mediate their immunosuppressive effect via the formation of functional *de-novo* iT_{reg}. Our results are in line with earlier *in-vivo* studies with bone-marrow MSC in animal models and a recent case report of MSC administration to renal transplant patients; these studies also observed proportional increases of T_{reg} [9,35,41,42]. However, as these groups did not investigate the T_{reg} origin and T_{reg} functionality, it is not clear whether the observed rises in T_{reg} percentages are a consequence of the *de-novo* formation of T_{reg} or a result of the expansion of existing nT_{reg}. We found that ASC mediate the generation of iT_{reg}

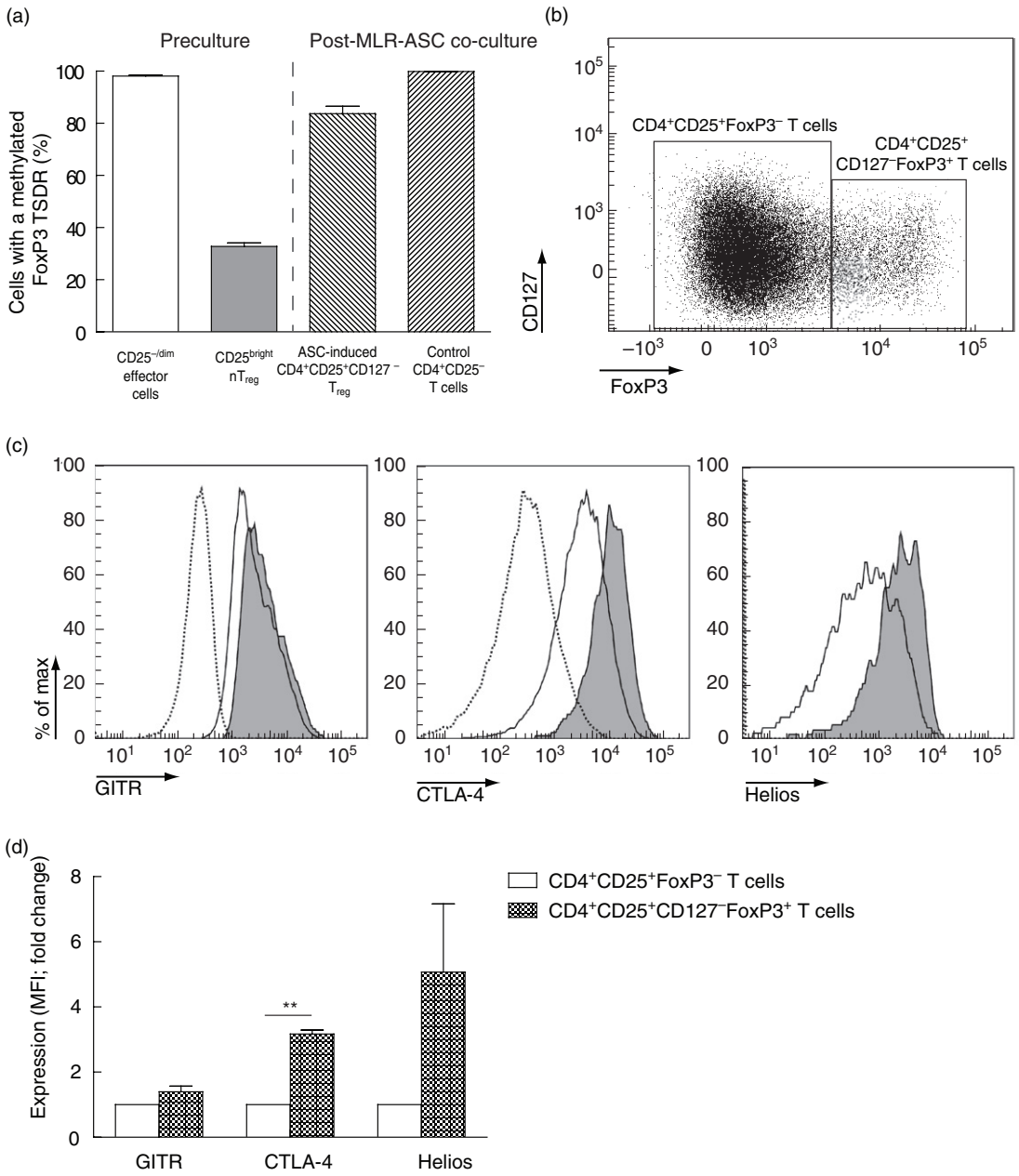

Fig. 4. Characterization of adipose-tissue derived mesenchymal stem cells (ASC)-induced $CD4^+CD25^+CD127^-$ regulatory T cells (T_{reg}). (a) Methylation analysis of the *FOXP3* gene T_{reg}-specific demethylated region (TSDR). $CD25^{-/dim}$ effector cells and $CD25^{bright}$ natural T_{reg} (nT_{reg}) were obtained from peripheral blood mononuclear cells (PBMC) by means of cell separation. $CD4^+CD25^-$ T cells and ASC-induced $CD4^+CD25^+CD127^-$ T_{reg} were isolated from lymphocyte populations by cell sorting after 7-day mixed lymphocyte reaction (MLR)–ASC co-cultures; co-cultures consisted of $CD25^{-/dim}$ effector cells, γ-irradiated allogeneic PBMC and ASC (1:40; ASC/effector cells). The methylation status of the *FOXP3* TSDR in the different cell populations was determined. The percentage of cells with a methylated TSDR was calculated using the ratio of amplified methylated TSDR copies and total TSDR copies. Results obtained from female PBMC donors were multiplied by 2; $n = 7$; six male, one female; mean ± standard error of the mean (s.e.m.). (b) Gating strategy to discriminate $CD4^+CD25^+CD127^-$forkhead box P3 (FoxP3)$^+$ T cells from $CD4^+CD25^+FoxP3^-$ T cells. A representative example for MLR–ASC co-culture (1:40; ASC/effector cells) is shown. (c) Expression of glucocorticoid-induced tumour necrosis factor receptor (TNFR)-related protein (GITR), cytotoxic T-lymphocyte antigen-4 (CTLA-4) and Helios. Flow cytometric analyses of protein expression by $CD4^+CD25^+FoxP3^-$ T cells (white histogram) and $CD4^+CD25^+CD127^-FoxP3^+$ T cells (grey histogram) are shown. Fluorescence minus one (FMO) controls are depicted as dotted histogram. Representative examples for MLR–ASC co-culture (1:40; ASC/effector cells) are shown. Data of multiple experiments are shown in d. (d). Expression of GITR, CTLA-4 and Helios by $CD4^+CD25^+FoxP3^-$ T cells (white bars) and $CD4^+CD25^+CD127^-FoxP3^+$ T cells (checkered bars). Protein expression is shown as fold changes of median fluorescence intensity (MFI) between $CD4^+CD25^+FoxP3^-$ T cells and $CD4^+CD25^+CD127^-FoxP3^+$ T cells. Expression levels of $CD4^+CD25^+FoxP3^-$ T cells were used as reference. $n = 3$, mean ± s.e.m.; paired *t*-test; $^{**}P < 0{\cdot}01$.

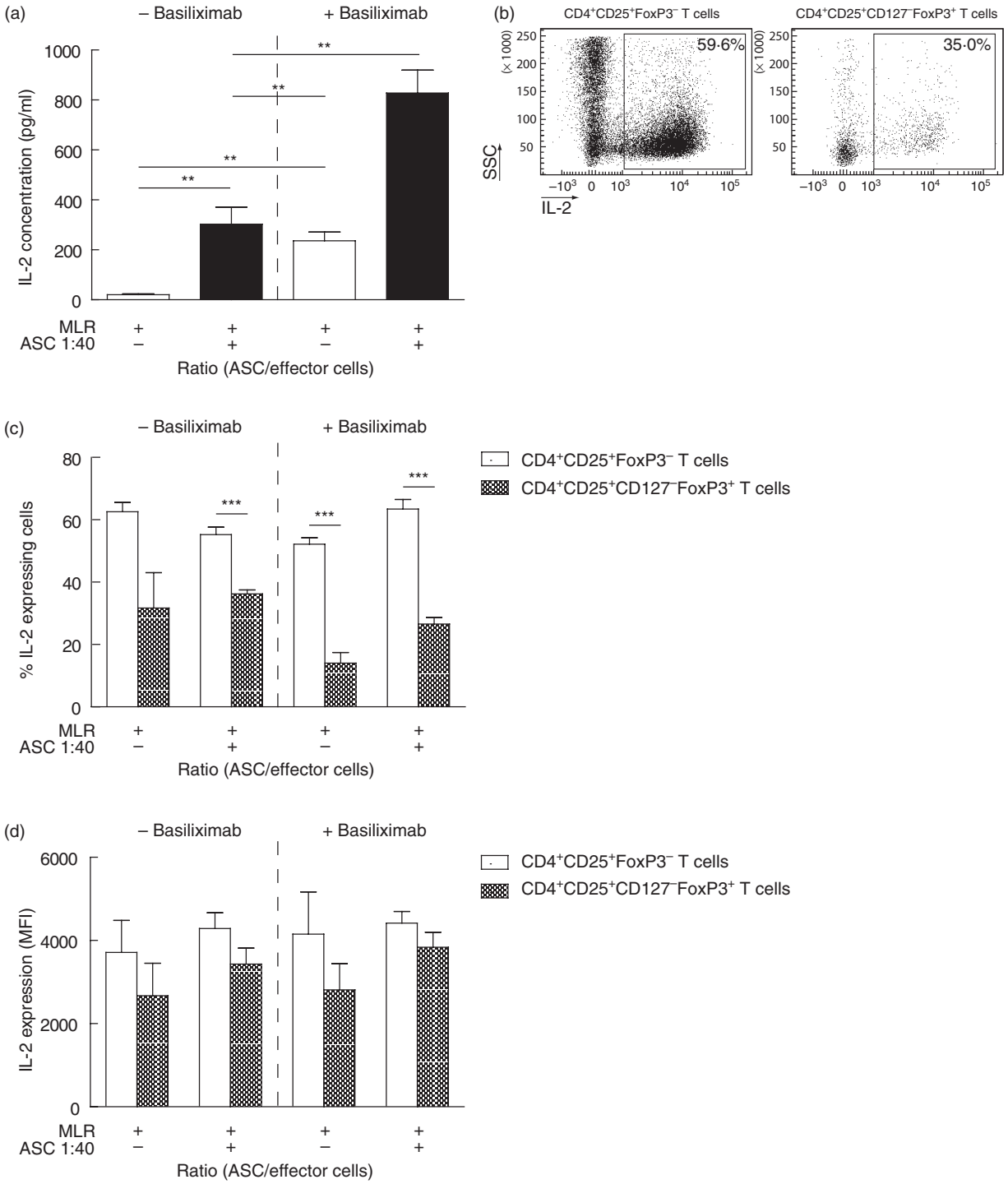

Fig. 5. Effect of mixed lymphocyte reaction (MLR) adipose-tissue-derived mesenchymal stem cells (ASC) co-culture and basiliximab on interleukin (IL)-2 expression. (a) IL-2 levels in cell culture supernatants. MLR (white bars) consisted of $CD25^{-/dim}$ effector cells stimulated with γ-irradiated allogeneic peripheral blood mononuclear cells (PBMC) and were performed for 7 days in the presence and absence of basiliximab. In co-cultures with MLR, ASC were used at a 1:40 ratio (ASC/effector cells; black bars). The IL-2 concentration in the cell culture supernatants was determined by cytometric bead array (CBA). $n = 6$, mean ± standard error of the mean (s.e.m.); paired *t*-test; ** $P < 0{\cdot}01$. (b) Percentage of IL-2-expressing cells within the $CD4^+CD25^+$ forkhead box P3 (FoxP3)$^-$ T cells and $CD4^+CD25^+CD127^-FoxP3^+$ T cells after 7-day MLR–ASC co-culture (representative examples are shown). (c) Data of multiple experiments showing the percentage of IL-2-expressing cells within the $CD4^+CD25^+FoxP3^-$ T cells (white bars) and $CD4^+CD25^+CD127^-FoxP3^+$ T cells (chequered bars); $n = 5$; mean ± s.e.m.; paired *t*-test; *** $P < 0{\cdot}001$. (d) Levels of expressed IL-2. Median fluorescence intensity (MFI); $n = 5$.

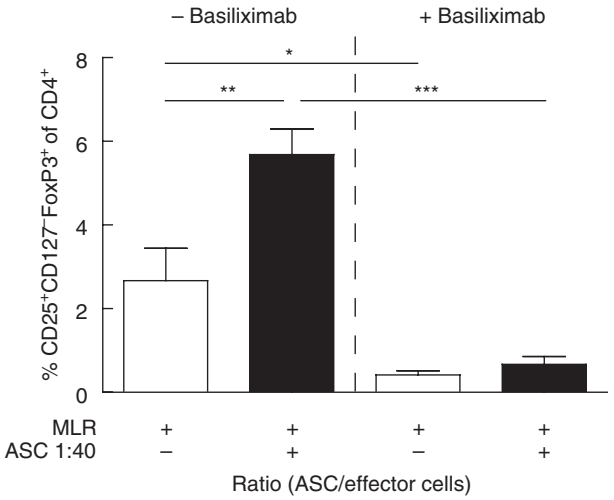

Fig. 6. Effect of basiliximab on the induction of $CD4^+CD25^+CD127^-$ forkhead box P3 $(FoxP3)^+$ regulatory T cells (T_{reg}). Mixed lymphocyte reaction (MLR) (white bars) consisted of $CD25^{-/dim}$ effector cells stimulated with γ-irradiated allogeneic peripheral blood mononuclear cells (PBMC) and were performed for 7 days. In MLR co-cultures adipose tissue-derived mesenchymal stem cells (ASC) were used at a 1:40 ratio (ASC/effector cells; black bars). In the absence and presence of basiliximab, the percentage of $CD25^+CD127^-FoxP3^+$ cells within the $CD4^+$ T cell population was determined by flow cytometry; $n = 6$, mean ± standard error of the mean; paired *t*-test; $^*P < 0{\cdot}05$; $^{**}P < 0{\cdot}01$; $^{***}P < 0{\cdot}001$.

from effector T cells and that these newly formed cells have immunosuppressive capacities. iT_{reg} also formed in MLR without ASC, but at lower numbers. While ASC-induced T_{reg} showed similar suppressive capacities to nT_{reg}, MLR-induced T_{reg} had a stronger inhibitory effect. The induction of a more potent immunosuppressive phenotype in these cells might be due to their generation under highly proinflammatory conditions. In the presence of ASC effector cell proliferation is reduced. Because of this milder environment higher numbers of less effective iT_{reg} are generated. Therefore, the suppressive strength of iT_{reg} might be proportional to the stimulus under which they are induced. Further, due to the presence of a few nT_{reg} in our initial effector T cell population we were able to infer that ASC also mediate an increase in nT_{reg}.

Although the first evidence of extrathymic conversion of conventional T cells into iT_{reg} was found almost a decade ago, no iT_{reg}-specific marker has yet been identified [43–45]. The only tool currently available to distinguish iT_{reg} from nT_{reg} is the determination of the methylation status of the TSDR. While nT_{reg} have a demethylated TSDR, this specific region of the *FOXP3* gene is methylated in iT_{reg} [37]. The high percentage of cells with a methylated TSDR in the ASC-induced T_{reg} fraction indicates that the vast majority of these cells originated from $CD25^{-/dim}$ effector cells. To characterize further the ASC-induced T_{reg} we investigated their expression of GITR, CTLA-4 and Helios. GITR expression was similar in both iT_{reg} and $CD4^+CD25^+FoxP3^-$ T cells. In contrast, iT_{reg} showed a tendency towards a higher Helios expression and expressed significantly higher CTLA-4 levels than $FoxP3^-$ T cells. It has been described that CTLA-4 expression is up-regulated upon binding of FoxP3 to the promoter of the *CTLA-4* gene [46–50]. Therefore, the observed difference in CTLA-4 expression between iT_{reg} and $FoxP3^-$ T cells can be attributed to their differing FoxP3 expression. Whether Helios is a potential marker for human iT_{reg} is an ongoing debate in the field, as conflicting results have been reported [51–53].

In search of possible underlying mechanisms involved in MSC-mediated iT_{reg} generation, it has been reported recently that programmed death ligand-1 (PD-L1), a protein expressed by MSC, promotes the differentiation of Th1 cells into T_{reg} [22,54]. Other molecules that were suggested to play a role in the induction of T_{reg} by MSC are IDO, prostaglandin E_2 (PGE_2), transforming growth factor (TGF)-β and haem oxygenase-1 (HO-1) [41,55–58]. In this study we focused on the role of IL-2 in ASC-mediated T_{reg} induction, as IL-2 drives T cell proliferation and, paradoxically, is also essential for tolerance induction by regulating nT_{reg} function [59]. We observed that in the presence of ASC, the IL-2 concentration in the cell culture supernatant increased. Because IL-2 is not expressed by ASC, the IL-2 surplus originated from the alloactivated effector cells. Upon T cell-receptor engagement and co-stimulation, activated effector T cells consume IL-2. During the inhibition of effector T cell proliferation by ASC, IL-2 concentrations in the cell culture supernatant rose. This indicates that although their proliferation is suppressed, effector T cells remain activated and continue to secrete IL-2. The diminished proliferation rate of effector T cells causes a reduced IL-2 consumption and hence a surplus of IL-2. High levels of IL-2 are instrumental for T_{reg} induction. In the presence of basiliximab, we found further accumulation of IL-2 in the supernatant. In its function as anti-rejection therapy in kidney transplant patients, basiliximab prevents the binding of IL-2 to its receptor and the subsequent uptake of IL-2. As a result, basiliximab inhibits T cell proliferation but also iT_{reg} generation, indicating that T_{reg} induction by ASC is IL-2 pathway-dependent. Surprisingly, IL-2 was expressed not only by $CD4^+CD25^+FoxP3^-$ T cells but also by a smaller percentage of immunosuppressive ASC-induced T_{reg}. Phenotypic adaptation of T_{reg} in response to the cytokines present in their environment is a known phenomenon [60]. The inhibition of T cell proliferation is not an exclusive effect of MSC, as other stromal cells share this characteristic [61,62] Hence, it is possible that these cells can also create an environment that favours iT_{reg} generation.

The graft-supporting effects of MSC in animal models and the positive results of MSC treatment for graft-*versus*-host disease (GVHD) in patients who underwent haematopoietic stem cell transplantation (HSCT) are strongly convincing [8,63]. The reported short lifespan of MSC after

infusion, however, indicates that MSC are only initiators of these effects. Long-term, MSC do not actively promote immunosuppression themselves. Nevertheless, they are able to pass on their immunosuppressive capabilities through the induction of functional *de-novo* T_{reg}, the expansion of nT_{reg} or possibly through other immune cells which remain to be identified.

Despite continuous efforts, the translation of the experimental success of T_{reg}-mediated immune regulation to its application in clinical settings proves difficult. In animal models, *ex-vivo*- or *in-vivo*-generated T_{reg} prevent type 1 diabetes, reduce the severity of experimental autoimmune encephalomyelitis (EAE), control the acute and chronic rejection of allografts and attenuate or prevent GVHD [64–70]. In humans, thus far, *ex-vivo*-expanded T_{reg} have been used only for the treatment of patients undergoing HSCT. In these few clinical studies, T_{reg} were able to reduce the incidence of GVHD or to prevent GVHD [71–73]. Due to the heterogeneity of the T_{reg} population and the lack of a specific marker for human T_{reg}, *ex-vivo* T_{reg} expansion bears the risk of contamination with effector T cells. Therefore, *in-vivo* induction of functional T_{reg} mediated by MSC represents a beneficial effect of MSC therapy in addition to its immunosuppressive effect on effector T cells. Once the functionality of MSC-induced T_{reg} has been confirmed in autoimmune disease patients and allograft recipients, strategies to enhance the MSC-mediated *in-vivo* generation of iT_{reg} may be considered. Possible approaches could be MSC treatment combined with low-dose IL-2 therapy or the use of rapamycin and rabbit anti-thymocyte globulin (rATG), anti-rejection drugs which were found to advance nT_{reg} expansion and to allow T_{reg} induction, respectively [70,74–76].

In conclusion, our study demonstrates that human adipose tissue-derived MSC induce T_{reg} from effector T cells and that these *de-novo* T_{reg} are immunosuppressive. In conjunction with the well-known MSC function of preventing immune cell proliferation, our findings encourage the advancement of MSC therapy into clinical development for autoimmunity, GVHD and allograft rejection.

Disclosure

The authors of this manuscript have no conflicts of interest to disclose.

References

1 Hoogduijn MJ, Crop MJ, Peeters AM *et al.* Human heart, spleen, and perirenal fat-derived mesenchymal stem cells have immunomodulatory capacities. Stem Cells Dev 2007; **16**:597–604.

2 Pittenger MF, Mackay AM, Beck SC *et al.* Multilineage potential of adult human mesenchymal stem cells. Science 1999; **284**:143–7.

3 Zuk PA, Zhu M, Ashjian P *et al.* Human adipose tissue is a source of multipotent stem cells. Mol Biol Cell 2002; **13**:4279–95.

4 Antonucci I, Stuppia L, Kaneko Y *et al.* Amniotic fluid as a rich source of mesenchymal stromal cells for transplantation therapy. Cell Transplant 2011; **20**:789–95.

5 Figueroa FE, Carrion F, Villanueva S, Khoury M. Mesenchymal stem cell treatment for autoimmune diseases: a critical review. Biol Res 2012; **45**:269–77.

6 Dominguez-Bendala J, Lanzoni G, Inverardi L, Ricordi C. Concise review: mesenchymal stem cells for diabetes. Stem Cells Transl Med 2012; **1**:59–63.

7 Bernardo ME, Fibbe WE. Safety and efficacy of mesenchymal stromal cell therapy in autoimmune disorders. Ann NY Acad Sci 2012; **1266**:107–17.

8 Le Blanc K, Frassoni F, Ball L *et al.* Mesenchymal stem cells for treatment of steroid-resistant, severe, acute graft-versus-host disease: a phase II study. Lancet 2008; **371**:1579–86.

9 Casiraghi F, Azzollini N, Cassis P *et al.* Pretransplant infusion of mesenchymal stem cells prolongs the survival of a semiallogeneic heart transplant through the generation of regulatory T cells. J Immunol 2008; **181**:3933–46.

10 Popp FC, Eggenhofer E, Renner P *et al.* Mesenchymal stem cells can induce long-term acceptance of solid organ allografts in synergy with low-dose mycophenolate. Transpl Immunol 2008; **20**:55–60.

11 Zografou A, Tsigris C, Papadopoulos O *et al.* Improvement of skin-graft survival after autologous transplantation of adipose-derived stem cells in rats. J Plast Reconstr Aesthet Surg 2011; **64**:1647–56.

12 Roemeling-van Rhijn M, Weimar W, Hoogduijn MJ. Mesenchymal stem cells: application for solid-organ transplantation. Curr Opin Organ Transplant 2012; **17**:55–62.

13 Krampera M, Cosmi L, Angeli R *et al.* Role for interferon-gamma in the immunomodulatory activity of human bone marrow mesenchymal stem cells. Stem Cells 2006; **24**:386–98.

14 Crop MJ, Baan CC, Korevaar SS *et al.* Inflammatory conditions affect gene expression and function of human adipose tissue-derived mesenchymal stem cells. Clin Exp Immunol 2010; **162**:474–86.

15 Bartholomew A, Sturgeon C, Siatskas M *et al.* Mesenchymal stem cells suppress lymphocyte proliferation *in vitro* and prolong skin graft survival *in vivo*. Exp Hematol 2002; **30**:42–8.

16 Corcione A, Benvenuto F, Ferretti E *et al.* Human mesenchymal stem cells modulate B-cell functions. Blood 2006; **107**:367–72.

17 Sotiropoulou PA, Perez SA, Gritzapis AD, Baxevanis CN, Papamichail M. Interactions between human mesenchymal stem cells and natural killer cells. Stem Cells 2006; **24**:74–85.

18 Aggarwal S, Pittenger MF. Human mesenchymal stem cells modulate allogeneic immune cell responses. Blood 2005; **105**:1815–22.

19 Jiang XX, Zhang Y, Liu B *et al.* Human mesenchymal stem cells inhibit differentiation and function of monocyte-derived dendritic cells. Blood 2005; **105**:4120–6.

20 Di Nicola M, Carlo-Stella C, Magni M *et al.* Human bone marrow stromal cells suppress T-lymphocyte proliferation induced by cellular or nonspecific mitogenic stimuli. Blood 2002; **99**:3838–43.

21 Crop MJ, Baan CC, Korevaar SS *et al.* Donor-derived mesenchymal stem cells suppress alloreactivity of kidney transplant patients. Transplantation 2009; **87**:896–906.

22 Augello A, Tasso R, Negrini SM *et al.* Bone marrow mesenchymal progenitor cells inhibit lymphocyte proliferation by activation of the programmed death 1 pathway. Eur J Immunol 2005; **35**:1482–90.

23 Groh ME, Maitra B, Szekely E, Koc ON. Human mesenchymal stem cells require monocyte-mediated activation to suppress alloreactive T cells. Exp Hematol 2005; **33**:928–34.

24 Deuse T, Stubbendorff M, Tang-Quan K *et al*. Immunogenicity and immunomodulatory properties of umbilical cord lining mesenchymal stem cells. Cell Transplant 2011; **20**:655–67.

25 Sato K, Ozaki K, Oh I *et al*. Nitric oxide plays a critical role in suppression of T-cell proliferation by mesenchymal stem cells. Blood 2007; **109**:228–34.

26 Nasef A, Mathieu N, Chapel A *et al*. Immunosuppressive effects of mesenchymal stem cells: involvement of HLA-G. Transplantation 2007; **84**:231–7.

27 Meisel R, Zibert A, Laryea M, Gobel U, Daubener W, Dilloo D. Human bone marrow stromal cells inhibit allogeneic T-cell responses by indoleamine 2,3-dioxygenase-mediated tryptophan degradation. Blood 2004; **103**:4619–21.

28 Hoogduijn MJ, Popp F, Verbeek R *et al*. The immunomodulatory properties of mesenchymal stem cells and their use for immunotherapy. Int Immunopharmacol 2010; **10**:1496–500.

29 Engela AU, Baan CC, Peeters AM, Weimar W, Hoogduijn MJ. Interaction between adipose-tissue derived mesenchymal stem cells and regulatory T cells. Cell Transplant 2012; **22**:41–54.

30 English K, Ryan JM, Tobin L, Murphy MJ, Barry FP, Mahon BP. Cell contact, prostaglandin E_2 and transforming growth factor beta 1 play non-redundant roles in human mesenchymal stem cell induction of $CD4^+CD25^{(high)}$ forkhead box $P3^+$ regulatory T cells. Clin Exp Immunol 2009; **156**:149–60.

31 Di Ianni M, Del Papa B, De Ioanni M *et al*. Mesenchymal cells recruit and regulate T regulatory cells. Exp Hematol 2008; **36**:309–18.

32 Gonzalez MA, Gonzalez-Rey E, Rico L, Buscher D, Delgado M. Adipose-derived mesenchymal stem cells alleviate experimental colitis by inhibiting inflammatory and autoimmune responses. Gastroenterology 2009; **136**:978–89.

33 Ge W, Jiang J, Baroja ML *et al*. Infusion of mesenchymal stem cells and rapamycin synergize to attenuate alloimmune responses and promote cardiac allograft tolerance. Am J Transplant 2009; **9**:1760–72.

34 Kavanagh H, Mahon BP. Allogeneic mesenchymal stem cells prevent allergic airway inflammation by inducing murine regulatory T cells. Allergy 2011; **66**:523–31.

35 Perico N, Casiraghi F, Introna M *et al*. Autologous mesenchymal stromal cells and kidney transplantation: a pilot study of safety and clinical feasibility. Clin J Am Soc Nephrol 2011; **6**:412–22.

36 Bilate AM, Lafaille JJ. Induced CD4+Foxp3+ regulatory T cells in immune tolerance. Annu Rev Immunol 2012; **30**:733–58.

37 Baron U, Floess S, Wieczorek G *et al*. DNA demethylation in the human FOXP3 locus discriminates regulatory T cells from activated FOXP3(+) conventional T cells. Eur J Immunol 2007; **37**:2378–89.

38 Eggenhofer E, Benseler V, Kroemer A *et al*. Mesenchymal stem cells are short-lived and do not migrate beyond the lungs after intravenous infusion. Front Immunol 2012; **3**:297.

39 Wieczorek G, Asemissen A, Model F *et al*. Quantitative DNA methylation analysis of FOXP3 as a new method for counting regulatory T cells in peripheral blood and solid tissue. Cancer Res 2009; **69**:599–608.

40 Livak KJ, Schmittgen TD. Analysis of relative gene expression data using real-time quantitative PCR and the 2(-Delta Delta C(T)) method. Methods 2001; **25**:402–8.

41 Ge W, Jiang J, Arp J, Liu W, Garcia B, Wang H. Regulatory T-cell generation and kidney allograft tolerance induced by mesenchymal stem cells associated with indoleamine 2,3-dioxygenase expression. Transplantation 2010; **90**:1312–20.

42 Casiraghi F, Azzollini N, Todeschini M *et al*. Localization of mesenchymal stromal cells dictates their immune or proinflammatory effects in kidney transplantation. Am J Transplant 2012; **12**:2373–83.

43 Furtado GC, Curotto de Lafaille MA, Kutchukhidze N, Lafaille JJ. Interleukin 2 signaling is required for CD4(+) regulatory T cell function. J Exp Med 2002; **196**:851–7.

44 Curotto de Lafaille MA, Lino AC, Kutchukhidze N, Lafaille JJ. CD25– T cells generate CD25+Foxp3+ regulatory T cells by peripheral expansion. J Immunol 2004; **173**:7259–68.

45 Curotto de Lafaille MA, Lafaille JJ. Natural and adaptive foxp3+ regulatory T cells: more of the same or a division of labor? Immunity 2009; **30**:626–35.

46 Wu Y, Borde M, Heissmeyer V *et al*. FOXP3 controls regulatory T cell function through cooperation with NFAT. Cell 2006; **126**:375–87.

47 Marson A, Kretschmer K, Frampton GM *et al*. Foxp3 occupancy and regulation of key target genes during T-cell stimulation. Nature 2007; **445**:931–5.

48 Zheng Y, Josefowicz SZ, Kas A, Chu TT, Gavin MA, Rudensky AY. Genome-wide analysis of Foxp3 target genes in developing and mature regulatory T cells. Nature 2007; **445**:936–40.

49 Ono M, Yaguchi H, Ohkura N *et al*. Foxp3 controls regulatory T-cell function by interacting with AML1/Runx1. Nature 2007; **446**:685–9.

50 Wing K, Onishi Y, Prieto-Martin P *et al*. CTLA-4 control over Foxp3+ regulatory T cell function. Science 2008; **322**:271–5.

51 Thornton AM, Korty PE, Tran DQ *et al*. Expression of Helios, an Ikaros transcription factor family member, differentiates thymic-derived from peripherally induced Foxp3+ T regulatory cells. J Immunol 2010; **184**:3433–41.

52 Akimova T, Beier UH, Wang L, Levine MH, Hancock WW. Helios expression is a marker of T cell activation and proliferation. PLoS ONE 2011; **6**:e24226.

53 Gottschalk RA, Corse E, Allison JP. Expression of Helios in peripherally induced Foxp3+ regulatory T cells. J Immunol 2012; **188**:976–80.

54 Amarnath S, Mangus CW, Wang JC *et al*. The PDL1–PD1 axis converts human TH1 cells into regulatory T cells. Sci Transl Med 2011; **3**:111ra20.

55 Tatara R, Ozaki K, Kikuchi Y *et al*. Mesenchymal stromal cells inhibit Th17 but not regulatory T-cell differentiation. Cytotherapy 2011; **13**:686–94.

56 Ghannam S, Pene J, Torcy-Moquet G, Jorgensen C, Yssel H. Mesenchymal stem cells inhibit human Th17 cell differentiation and function and induce a T regulatory cell phenotype. J Immunol 2010; **185**:302–12.

57 Tasso R, Ilengo C, Quarto R, Cancedda R, Caspi RR, Pennesi G. Mesenchymal stem cells induce functionally active T-regulatory lymphocytes in a paracrine fashion and ameliorate experimental autoimmune uveitis. Invest Ophthalmol Vis Sci 2012; **53**:786–93.

58 Mougiakakos D, Jitschin R, Johansson CC, Okita R, Kiessling R, Le Blanc K. The impact of inflammatory licensing on heme oxygenase-1-mediated induction of regulatory T cells by human mesenchymal stem cells. Blood 2011; **117**:4826–35.

59 Cheng G, Yu A, Malek TR. T-cell tolerance and the multifunctional role of IL-2R signaling in T-regulatory cells. Immunol Rev 2011; **241**:63–76.
60 Koch MA, Tucker-Heard G, Perdue NR, Killebrew JR, Urdahl KB, Campbell DJ. The transcription factor T-bet controls regulatory T cell homeostasis and function during type 1 inflammation. Nat Immunol 2009; **10**:595–602.
61 Haniffa MA, Wang XN, Holtick U *et al*. Adult human fibroblasts are potent immunoregulatory cells and functionally equivalent to mesenchymal stem cells. J Immunol 2007; **179**:1595–604.
62 Jones S, Horwood N, Cope A, Dazzi F. The antiproliferative effect of mesenchymal stem cells is a fundamental property shared by all stromal cells. J Immunol 2007; **179**:2824–31.
63 Le Blanc K, Rasmusson I, Sundberg B *et al*. Treatment of severe acute graft-versus-host disease with third party haploidentical mesenchymal stem cells. Lancet 2004; **363**:1439–41.
64 Daniel C, Weigmann B, Bronson R, von Boehmer H. Prevention of type 1 diabetes in mice by tolerogenic vaccination with a strong agonist insulin mimetope. J Exp Med 2011; **208**:1501–10.
65 Kohm AP, Carpentier PA, Anger HA, Miller SD. Cutting edge: CD4+CD25+ regulatory T cells suppress antigen-specific autoreactive immune responses and central nervous system inflammation during active experimental autoimmune encephalomyelitis. J Immunol 2002; **169**:4712–6.
66 Bushell A, Wood K. GITR ligation blocks allograft protection by induced CD25+CD4+ regulatory T cells without enhancing effector T-cell function. Am J Transplant 2007; **7**:759–68.
67 Nadig SN, Wieckiewicz J, Wu DC *et al*. *In vivo* prevention of transplant arteriosclerosis by *ex vivo*-expanded human regulatory T cells. Nat Med 2010; **16**:809–13.
68 Issa F, Hester J, Goto R, Nadig SN, Goodacre TE, Wood K. *Ex vivo*-expanded human regulatory T cells prevent the rejection of skin allografts in a humanized mouse model. Transplantation 2010; **90**:1321–7.
69 Ermann J, Hoffmann P, Edinger M *et al*. Only the CD62L+ subpopulation of CD4+CD25+ regulatory T cells protects from lethal acute GVHD. Blood 2005; **105**:2220–6.
70 Shin HJ, Baker J, Leveson-Gower DB, Smith AT, Sega EI, Negrin RS. Rapamycin and IL-2 reduce lethal acute graft-versus-host disease associated with increased expansion of donor type CD4+CD25+Foxp3+ regulatory T cells. Blood 2011; **118**:2342–50.
71 Trzonkowski P, Bieniaszewska M, Juscinska J *et al*. First-in-man clinical results of the treatment of patients with graft versus host disease with human *ex vivo* expanded CD4+CD25+CD127– T regulatory cells. Clin Immunol 2009; **133**:22–6.
72 Brunstein CG, Miller JS, Cao Q *et al*. Infusion of *ex vivo* expanded T regulatory cells in adults transplanted with umbilical cord blood: safety profile and detection kinetics. Blood 2011; **117**:1061–70.
73 Di Ianni M, Falzetti F, Carotti A *et al*. Tregs prevent GVHD and promote immune reconstitution in HLA-haploidentical transplantation. Blood 2011; **117**:3921–8.
74 Koreth J, Matsuoka K, Kim HT *et al*. Interleukin-2 and regulatory T cells in graft-versus-host disease. N Engl J Med 2011; **365**:2055–66.
75 Battaglia M, Stabilini A, Roncarolo MG. Rapamycin selectively expands CD4+CD25+FoxP3+ regulatory T cells. Blood 2005; **105**:4743–8.
76 Sewgobind VD, van der Laan LJ, Kho MM *et al*. Characterization of rabbit antithymocyte globulins-induced CD25+ regulatory T cells from cells of patients with end-stage renal disease. Transplantation 2010; **89**:655–66.